metals

Article

Physical Experiments and Numerical Simulations of the Influence of Turbulence Inhibitors and the Position of Ladle Shroud on the Steel Flow in an Asymmetric Five-Strand Tundish

Josef Walek [1,*], Markéta Tkadlečková [2], Marek Velička [3], Mario Machů [3], Jiří Cupek [1], Tomáš Huczala [2], Jiří Cibulka [2], Jan Růžička [3] and Karel Michalek [1]

1 Department of Metallurgical Technologies, Faculty of Materials Science and Technology, VSB—Technical University of Ostrava, 17. listopadu 2172/15, 70800 Ostrava, Czech Republic; jiri.cupek@vsb.cz (J.C.); karel.michalek@vsb.cz (K.M.)
2 TŘINECKÉ ŽELEZÁRNY, a.s., Průmyslová 1000, Staré Město, 73961 Třinec, Czech Republic; marketa.tkadleckova@trz.cz (M.T.); tomas.huczala@trz.cz (T.H.); jiri.cibulka@trz.cz (J.C.)
3 Department of Thermal Engineering, Faculty of Materials Science and Technology, VSB—Technical University of Ostrava, 17. listopadu 2172/15, 70800 Ostrava, Czech Republic; marek.velicka@vsb.cz (M.V.); mario.machu@vsb.cz (M.M.); jan.ruzicka1@vsb.cz (J.R.)
* Correspondence: josef.walek@vsb.cz; Tel.: +420-597323534

Abstract: The submitted article deals with the use of physical and numerical modelling to study the process of the steel flow in an asymmetric five-strand tundish that continuously casts steel. For the purposes of physical modelling, a 1:4-scale plexiglass model was used as the operating tundish, and for numerical modelling, the geometry of the operating tundish was created on a 1:1 scale. A model liquid (water) was used in the physical modelling of the melt flow process, while liquid steel was used as the standard flowing medium in the numerical modelling. We assessed the relevant operating parameters influencing the characteristics of the flow of the bath in the tundish—the shape of the turbulence inhibitor, the position of the ladle shroud in relation to the turbulence inhibitor and the distance between the ladle shroud orifice and the bottom of the turbulence inhibitor. The preliminary results show that optimal steel flow characteristic results are achieved by using the TI3-C configuration. The results from both modelling methods achieved the same characteristics, therefore verifying the results of each other and demonstrating that when taken together, the results of physical and numerical modelling can be considered sufficiently informative.

Keywords: tundish; turbulence inhibitor; steel flow; retention time; modelling

check for updates

Citation: Walek, J.; Tkadlečková, M.; Velička, M.; Machů, M.; Cupek, J.; Huczala, T.; Cibulka, J.; Růžička, J.; Michalek, K. Physical Experiments and Numerical Simulations of the Influence of Turbulence Inhibitors and the Position of Ladle Shroud on the Steel Flow in an Asymmetric Five-Strand Tundish. *Metals* **2023**, *13*, 1821. https://doi.org/10.3390/met13111821

Academic Editor: Jiehua Li

Received: 5 September 2023
Revised: 27 September 2023
Accepted: 22 October 2023
Published: 29 October 2023

1. Introduction

During the continuous casting of steel, a tundish is placed between the ladle and the mould and is one of the most important technological nodes in the process because it affects the stability of the casting process and the quality of the continuous cast preform. The tundish primarily serves as a reservoir for liquid steel during sequential casting, providing sufficient time for ladle changes without having to prematurely interrupt the flow of liquid steel into the molds [1–3].

The tundish can be used as a flow-through reactor for bath mixing, as, to a certain extent, it is still possible to modify the properties of the cast steel at this point. One of the basic functions of the tundish is to distribute liquid steel between the individual casting strands. The even distribution of steel needs to be ensured so that the physical and chemical properties of the steel are approximately the same in all strands. The steel in the individual casting strands should have the same temperature, the same chemical structure and the same purity in terms of the content of non-metallic inclusions. These individual properties are closely related to the characteristics of the steel flow in the tundish. The steel flow is influenced by the internal arrangements of the tundish, and various objects are inserted into the tundish in order to optimize the characteristics of the steel flow in a suitable way. Optimizing the bath flow in the tundish is an important part of the efficient operation of every continuous casting. It is clear from an analysis of the literature that at present, the most common objects inserted into the tundish to improve the characteristics of the flow include turbulence inhibitors, which are inserted under the ladle shroud, baffles, dams and weirs, and argon stirring elements [2–6].

Turbulence inhibitors prevent steel spattering when filling an empty tundish. They significantly reduce the turbulence intensity of the input pouring current. They direct the flow of steel, create an area for the steel to flow through the plug flow and assist the flotation of inclusions. Turbulence inhibitors increase and equalize the retention time of the bath in the tundish, increase the proportion of volume with plug flow and eliminate short-circuit flow. The use of the turbulence inhibitors can not only reduce the amount of entrained slag, but also reduce the reoxidation of steel during ladle replacement [7–12].

Baffles fundamentally change the characteristics of the steel flow in the tundish due to their holes. They direct the flow of the bath towards the surface of the steel in the tundish, thereby creating more suitable conditions for some non-metallic inclusions to float, while the adsorption process allows others to adhere to the partition surface. Baffles create thermal homogenization in the tundish. They increase the resistance of the steel flow, thereby increasing the minimum retention time. Baffles eliminate short-circuit flow, increase the proportion of steel volume with plug flow and reduce dead volume [13–17].

Dams and weirs aim to extend and equalize retention times, and eliminate dead volumes and short-circuit flow in the tundish. Dams and weirs can improve the temperature and chemical homogeneity of the steel in the tundish. The use of a weir alone could cause short-circuit flow and the formation of dead volumes. Therefore, it is advisable to combine it with a dam, which should eliminate the short-circuit flow issue. Dams are mainly used to direct the liquid flow towards the metal–slag interface to increase the retention time of the liquid steel in the tundish [18–20].

The argon stirring element in the bottom of the tundish favorably affects the characteristics of the flow. It has a positive effect on the proportion of volume with plug flow and on the reduction of the transition zone. It supports the temperature and chemical homogenization of steel in the tundish. Blown argon acts as a screen that directs the steel flow, thereby greatly promoting the floatation of inclusions and eliminating short-circuit flow. It is important to ensure the appropriate positioning of the argon stirring element and the appropriate flow of argon [21,22].

The optimization of the metallurgical processes of steel flow in the tundish is difficult under operating conditions. Therefore, in laboratory conditions, modelling is used, where the original prototype is replaced by a physical or numerical model. In physical modelling, the real system is replaced by a tangible physical model that is as identical to the behavior of the real system as possible. The purpose of physical modelling is the targeted utilization of the similarities between the processes that take place within the actual device and its model. In this method, both the prototype and the model have the same physical structure and purpose, and these similarities ensure that the results from the model can be applied to the prototype. One of the advantages of physical modelling is the ability to visualize the processes taking place in the real system. The second method of modelling is numerical modelling, which is advantageous for simulating metallurgical processes because, unlike physical modelling, extreme boundary conditions can be simulated. Unlike physical modelling, numerical modelling has a different physical structure to the prototype. The original technological process is replaced by a mathematical model that describes the given event through partial differential equations and continuity equations. This type of modelling is a useful tool, as the results achieved on the model can predict real system behavior during various process changes. Comparing the results of physical and numerical modelling is an effective and optimal variant of model research [2,23–28].

The aim of the present article is to evaluate the methodology of laboratory experiments and simulations, namely, physical and numeral modelling, regarding the characteristics of steel flow in a tundish.

2. Materials and Methods

2.1. Experimental Conditions for Physical Modelling

Physical experiments investigating the characteristics of steel flow in a tundish were performed in the Laboratory of Physical and Numerical Modelling at the Department of Metallurgical Technologies, Faculty of Materials Science and Technology, at the VSB—Technical University of Ostrava.

The physical model, consisting of a ladle shroud, individual turbulence inhibitors and molds, was made of transparent organic glass (plexiglass) on a geometric scale of 1:4 to the operating tundish. This physical model also included two ladles to ensure the flow of water into the tundish through the ladle shroud. Each casting strand was equipped with a stopper rod, which, if necessary, could regulate the flow from the tundish to the molds. The casting strands were equipped with submerge entry nozzles at the same level as the steel in the molds. Figure 1 shows the schema of the ladle, tundish and molds. Figure 2 shows a general overview of the experimental equipment.

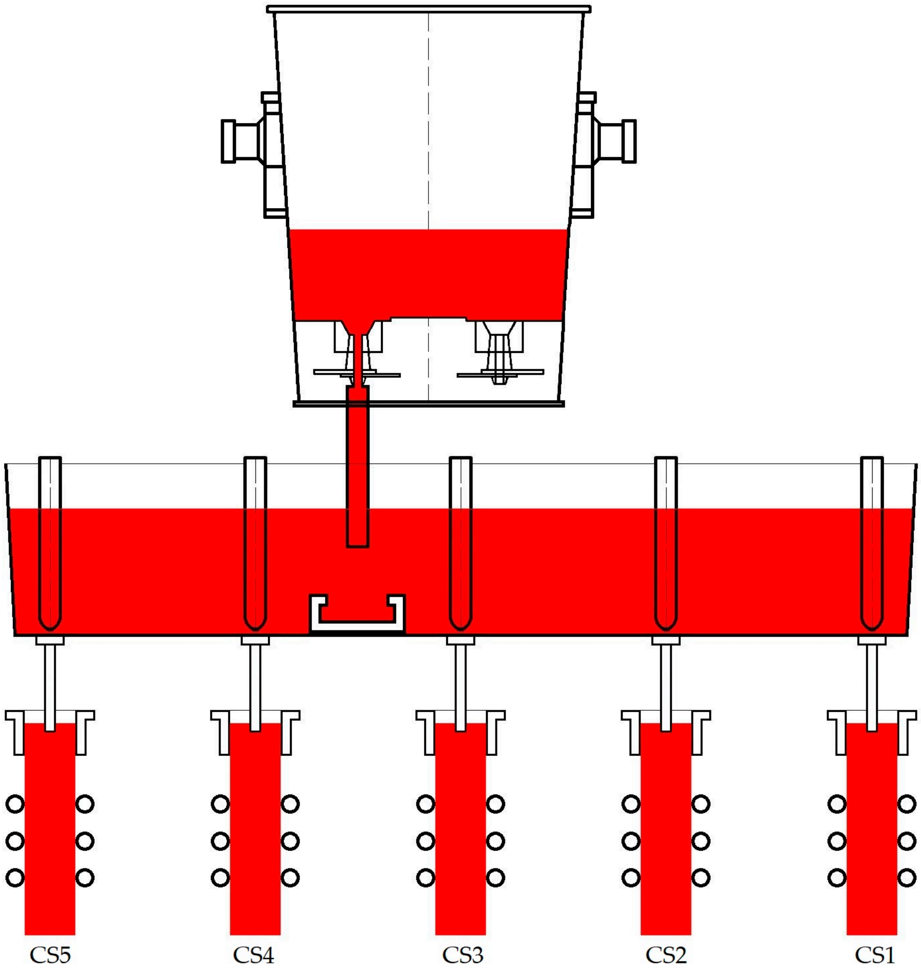

Figure 1. Schema of the ladle, tundish and molds.

Figure 2. Experimental device—the physical model of an asymmetric five-strand tundish.

The characteristics of the steel flow in the tundish were simulated in the physical model using a model liquid (water). The main advantages of using water are primarily its low cost, good availability and its physical properties, which are similar to liquid steel. The kinematic viscosities of liquid steel and water can be considered to be very similar. Table 1 shows the basic parameters of the prototype and the model.

Table 1. Basic parameters of the prototype and the model.

Symbol	Parameter	Prototype	Model
V	Volume of the bath in the tundish [m^3]	4.64	37.12×10^{-3}
m	Weight of the bath in the tundish [kg]	32,480	37.04
T_k	Average temperature of the bath [K]	1520 + 273	20 + 273
ρ_k	Average density of the bath [$kg \cdot m^{-3}$]	7000	998
ν_k	Kinematic viscosity of the bath [$m^2 \cdot s^{-1}$]	0.913×10^{-6}	1.02×10^{-6}
g	Gravitational acceleration [$m \cdot s^{-2}$]	9.81	9.81
p_v	Pressure above the bath surface [$kg \cdot m^{-1} \cdot s^{-2}$]	98.06×10^3	98.06×10^3
L_1	Internal length of the tundish at the plane of the bottom [m]	6.387	1.597
L_2	Distance between SEN [m]	1.5	0.375
D_1	Inner diameter of the ladle shroud [m]	0.085	0.021
H_1	Bath height appropriate to weight m [m]	0.925	0.231
H_2	Distance of the ladle shroud orifice from the bottom of the TI [m]	0.525	0.131
$Q_{m, k}$	Mass flow rate of the bath to the tundish [$kg \cdot min^{-1}$]	2779	12.39
$Q_{v, k}$	Volumetric flow rate of the bath to the tundish [$l \cdot min^{-1}$]	397	12.41
$Q_{v, kr}$	Volumetric flow rate on the each SEN [$l \cdot min^{-1}$]	79.4	2.48

The physical model was equipped with a measuring center, to measure the conductivity and temperature of the model and its regulatory system, as well as volumetric flow meters, and conductivity and temperature probes, which were placed in the ladle shroud and in each submerge entry nozzle. The conductivity probes measured conductivity continuously using two opposite platinum electrodes, and the temperature probes measured in the range 0–60 °C using a temperature Ni resistance sensor.

Laboratory experiments were conducted in accordance with the theory of similarity between the prototype and the model, based on the identity of Froude's criterion. It was necessary to ensure, in particular, geometrical similarity between the prototype and its model, and the dynamic similarity of fluid flow through each. Before each experiment, the relevant internal arrangement of the tundish was set up, i.e., inserting the relevant turbulence inhibitor into the tundish and setting the position and height of the ladle shroud relative to the turbulence inhibitor, until a steady state of casting was reached. Subsequently, the experiment itself was started and an impulse of 50 mL of aqueous KCl solution was injected into the ladle shroud. The response to the impulse was monitored by the submerge entry nozzles, particularly the change in conductivity and temperature. As the results of each experiment were affected by minor flow fluctuations in the tundish, each experiment was repeated three times to ensure the reproducibility of the results. If a discrepancy was noted between the results, further experiments were performed until three matching results were attained. For further evaluation, the mean of all three correct measurements was calculated.

The main aim of physical modelling was to achieve insight into the influence of relevant parameters on the characteristics of steel flow in the tundish, in particular:

- The shape of the turbulence inhibitor;
- The position of the ladle shroud in relation to the turbulence inhibitor.

Three variants of turbulence inhibitor were used for modelling, referred to as TI1 (i.e., turbulence inhibitor 1), TI2 and TI3 (see Figure 3). TI1 was a basic square variant, located at the back wall of the tundish; TI2 was a rectangular variant and extended over the entire width of the tundish; and TI3 was a variant TI2 with a convex bottom.

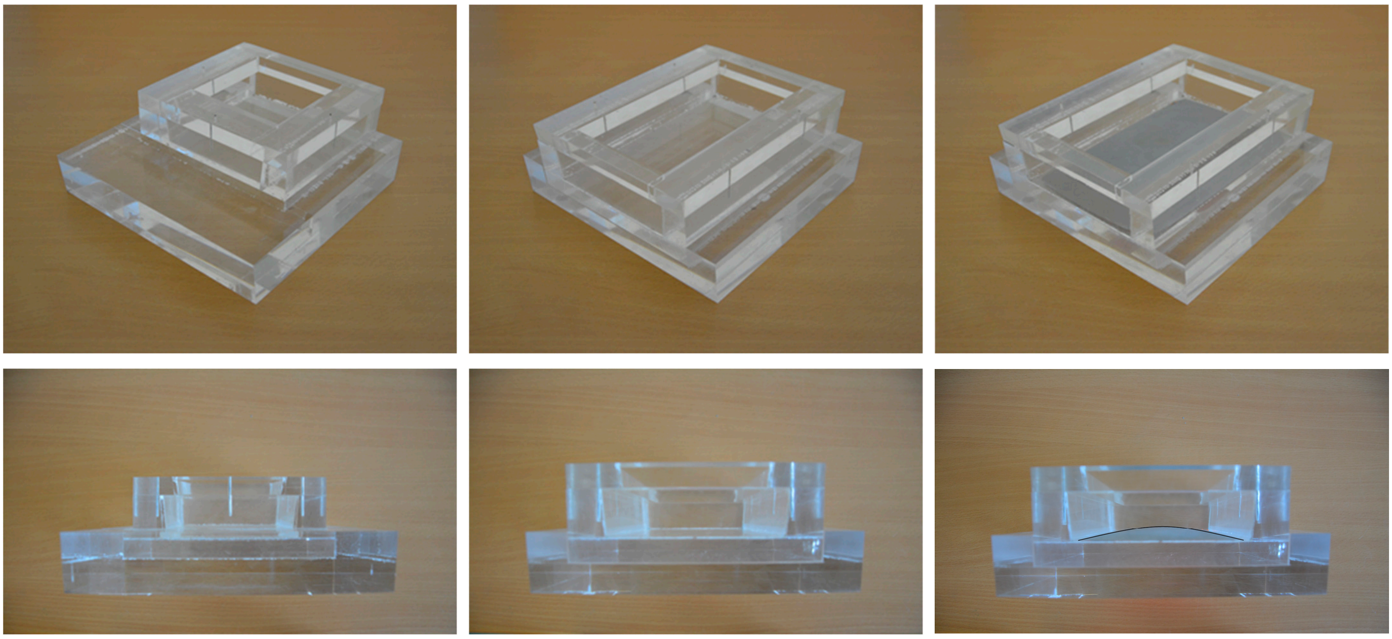

(**a**) (**b**) (**c**)

Figure 3. Variants of turbulence inhibitors used for physical modelling: (**a**) TI1; (**b**) TI2; (**c**) TI3.

The individual turbulence inhibitors were located in the tundish between the third and fourth casting strands (see Figure 4). The other monitored parameter, based on operational cases, was the position of the ladle shroud in relation to the turbulence inhibitor (see Figure 4).which were based on operational cases

(**a**)

(**b**)

(**c**)

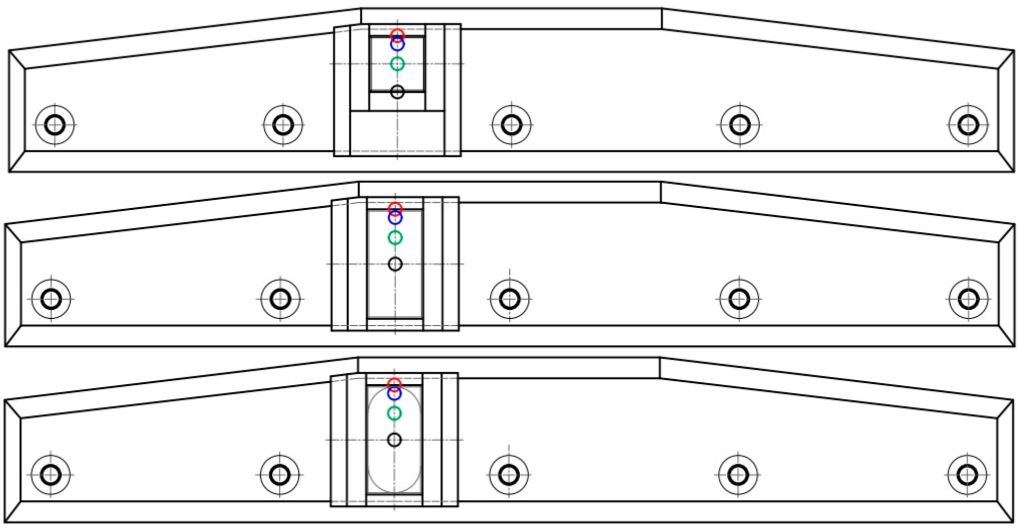

Figure 4. Internal arrangement of the tundish model including the individual positions of the ladle shroud for the individual turbulence inhibitors: (**a**) TI1-R1, R2, C, F1; (**b**) TI2-R1, R2, R3, C; (**c**) TI3-R1, R2, R3, C.

The positions of the ladle shroud in relation to the turbulence inhibitor in the model were as follows:

- Rear position 1 (R1)—identical for all variants;
- Rear position 2 (R2)—identical for all variants;
- Center position (C)—for TI1; Rear position 3 (R3) for TI2 and TI3;
- Front position 1 (F1)—for TI1; identical to Center position (C) for the TI2 and TI3.

2.2. Experimental Conditions for Numerical Modelling

As part of numerical modelling, parallel numerical simulations were performed in the CFD (Computational Fluid Dynamics) environment of the ANSYS Fluent program, version 19.2, which is part of the ANSYS Workbench software package. Numerical simulations aimed to verify the results of the physical modelling for selected variants. Variants with all types of the turbulence inhibitors, TI1, TI2 and TI3, were chosen for verification. The ladle shroud was in its central position, i.e., always above the geometric center of the respective turbulence inhibitor (position C). Figure 5 shows the 3D geometry of the tundish using TI3. For the numerical simulations, a tundish model was created at a scale of 1:1. The components of the tundish model were the appropriate turbulence inhibitor, ladle shroud, stopper rods and outlet nodes, including the submerge entry nozzles.

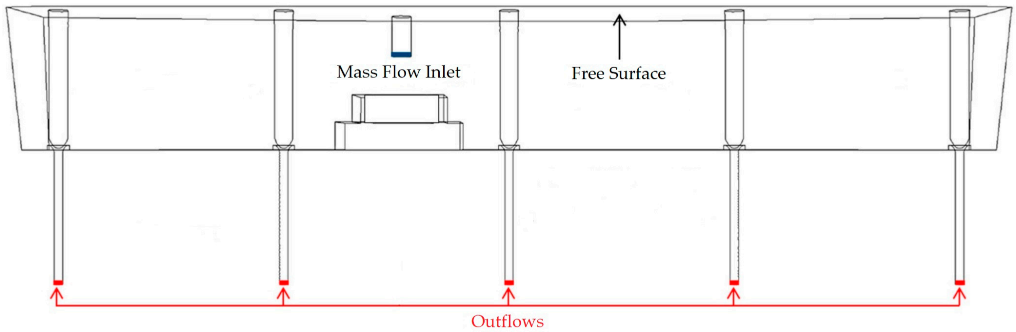

Figure 5. 3D geometry of the modelled area using TI3.

This created and defined geometry was subsequently imported into the meshing preprocessor environment, where a regular structured mesh was generated using the cut cell method. After creating the geometry and generating the computational mesh, the model was defined in Fluent. The standard k-epsilon turbulence model was chosen for the calculation of the steady flow field, taking into account the characteristics of the steel flow in the tundish. A standard wall function was defined on the walls of the tundish. Subsequently, the material properties of the following mediums were defined. To verify the results from the physical experiments, steel was simulated as a material in the numerical simulations. The thermophysical properties of steel were defined as a function of temperature for three values using a linear function. The defined thermophysical properties of steel are shown in the Table 2.

Table 2. Thermophysical properties of steel for numerical simulations.

Temperature (K)	**Density ($kg \cdot m^{-3}$)**	**Specific Heat ($J \cdot kg^{-1} \cdot K^{-1}$)**	**Thermal Conductivity ($W \cdot m^{-1} \cdot K^{-1}$)**	**Viscosity ($kg \cdot m^{-1} \cdot s^{-1}$)**
1793	6970	821	35	0.0055
1773	6985	813	35	0.0057
1753	7001	805	35	0.0059

In the next step, the boundary conditions were set. The operating conditions of the numerical simulations were also set within the boundary conditions. Values for heat loss through the walls of the tundish were set based on the literature [29,30]. The defined boundary conditions are listed in the Table 3. Calculations for the characteristics of the flow in the tundish basin took place in SW ANSYS Fluent and were solved by the numerical finite volume method. In order to achieve a convergent calculation solution, which is the goal in numerical simulations, it was necessary to determine the sizes of the residuals and the number of iterations. For the transient calculation, it was also necessary to determine the time step size, the number of time steps and the maximum number of iterations per time step.

Table 3. Model setup boundary conditions for numerical simulations.

Parameter	Value
Mass flow rate of the steel through the ladle shroud [$kg{\cdot}s^{-1}$]	46.32
Casting temperature [K]	1773
Turbulence intensity [%]	10
Hydraulic diameter [m]	0.085
Heat flux of the free surface [$W{\cdot}m^{-2}$]	15,000
Heat flux through the walls of the tundish [$W{\cdot}m^{-2}$]	2500
Gravity [$m{\cdot}s^{-2}$]	−9.81
Operating pressure [Pa]	101,325
Operating temperature [K]	1773

3. Results and Discussion

The evaluation of the physical experiments was carried out in three phases. In the first phase, retention time results were compared; in the second phase, the results were compared on the basis of the distribution of individual volumes in the tundish; and in the last evaluation phase, visualization photos were taken, with injected dye showing the characteristics of the bath flow in the tundish. As the results of each trial were affected by minor flow fluctuations in the tundish, each trial was repeated three times to ensure the reproducibility of the results. For further assessment, the mean of all three correct measurements was calculated.

The characteristics of steel flow in the tundish were studied as part of numerical simulations. A basic calculation of steady flow was performed in order to obtain a stationary flow field of the steel in the tundish. With this steady flow field, a transient calculation of RTD curves was subsequently performed using the species model.

3.1. Evaluation Methodology of the Physical Experiments

In the case of tundish metallurgy, it is important to know the amount of time a certain element of the melt spends in the tundish. The aim is to achieve characteristics that allow each element of the melt to stay in the tundish for as long as possible. The period of time that a certain part of the steel stays in the tundish is referred to as the retention time. The distribution of retention times is referred to as the RTD (residence time distribution). Retention times were determined by the conductivity method, which uses the differences in the conductivity of liquids. An aqueous solution of KCl, which is characterized by ionic conductivity, was used as an indicator medium in the individual experiments. The conductivity was measured with a conductivity probe at the input and output points of the tundish. The calculated results formed RTD C-curves [2].

The evaluation of the experiments was based on the measured data from the RTD curves. The minimum (c_{min}) and maximum (c_{max}) concentrations were determined from the measured course of the concentration change. From this, the dimensionless concentrations were calculated [2].

$$\bar{c} = (c - c_{min})/(c_{max} - c_{min}) \tag{1}$$

The theoretical average retention time was calculated using the liquid volume in the tundish and the volumetric liquid flow rate through the tundish [2].

$$\bar{\tau} = V/Q_V \tag{2}$$

The theoretical retention time considers a steady state when the volumetric liquid flow rate input into the tundish is the same as the volumetric liquid flow rate output. Since the steel flow in a multi-strand asymmetric tundish is associated with a dispersion of retention times, it was necessary to calculate the real retention time in order to evaluate the bath flow in the tundish [2].

$$\bar{\tau}_{real} = \left(\int c{\cdot}\tau{\cdot}d\tau\right)/\left(\int c{\cdot}d\tau\right) \tag{3}$$

Furthermore, the minimum retention time (τ_{min}) was determined from the measured course of the concentration change, which was defined as the time of the first appearance of the marker at the output, and the maximum retention time (τ_{max}), which was the time it took to reach maximum concentration at the output of the tundish. The coefficient of variation (v) was determined from the retention times, which indicates the variability of the retention times in the individual casting strands. The coefficient of variation is expressed as the quotient of the standard deviation and the mean [2].

$$v = \left(s/\bar{x} \cdot 100\right) \tag{4}$$

The tundish was assessed as a whole and the non-uniformity of the flow was evaluated according to the values of the individual minimum retention times and the appropriate coefficients of variation. The higher the coefficient of variation, the less equal the minimum retention times were, resulting in large differences. This condition is not optimal. The aim is to achieve the highest possible minimum retention times and, at the same time, low coefficients of variation. The obtained retention times can be used to calculate parameters that further refine the characteristics of the flow in the tundish. The total volume of the tundish basin was separated into three parts: mixed volume (V_m), volume with plug flow (V_p) and dead volume (V_d), all of which have different flow characteristics [2]. In the mixed volume area, there was an intensive mixing of steel, which was caused by the kinetic energy of the input casting current. The proportion of the mixed volume in the tundish was always ensured. Only during the replacement of casting ladles during sequential casting, when the supply of steel to the tundish is interrupted, does the mixed volume drop to zero. The proportion of mixed volume in the tundish was determined as an addition to the total volume [2].

$$(V_m/V) + (V_p/V) + (V_d/V) = 1 \tag{5}$$

This mixed volume area was followed by the area with plug flow, which was uniform with the bath flow, where no element of the melt overtakes another element. In this volume, the steel flow already had a laminar characteristic, and therefore more favorable conditions were created for the floating of inclusions [2].

$$\left(V_p/V\right) = \left(\tau_{min}/\bar{\tau}\right) \tag{6}$$

The third volume area of the tundish was the so-called dead volume. In this area, the steel flows very slowly and the melt has twice the average retention time. The dead volume reduces the active volume of the tundish, thus shortening the retention time of the steel flow. Local solidification of steel can occur in this area [2].

$$(V_d/V) = 1 - \left(\bar{\tau}_{real}/\bar{\tau}\right) \tag{7}$$

3.2. Evaluation of the Flow Characteristics from the Physical Modelling

Since the input to the tundish is positioned between casting strands 3 and 4, it is important that the highest possible minimum retention times for these strands are achieved, in order to eliminate short-circuit flow. The measured characteristics RTD C-curves show the dependence of the impulse change of concentration on time, the ladle shroud and all five casting strands for the selected variants, as can be seen in Figure 6. All measured and calculated flow characteristics are summarized in the Table 4. For better clarity, the flow characteristics are graphically displayed in Figures 7 and 8.

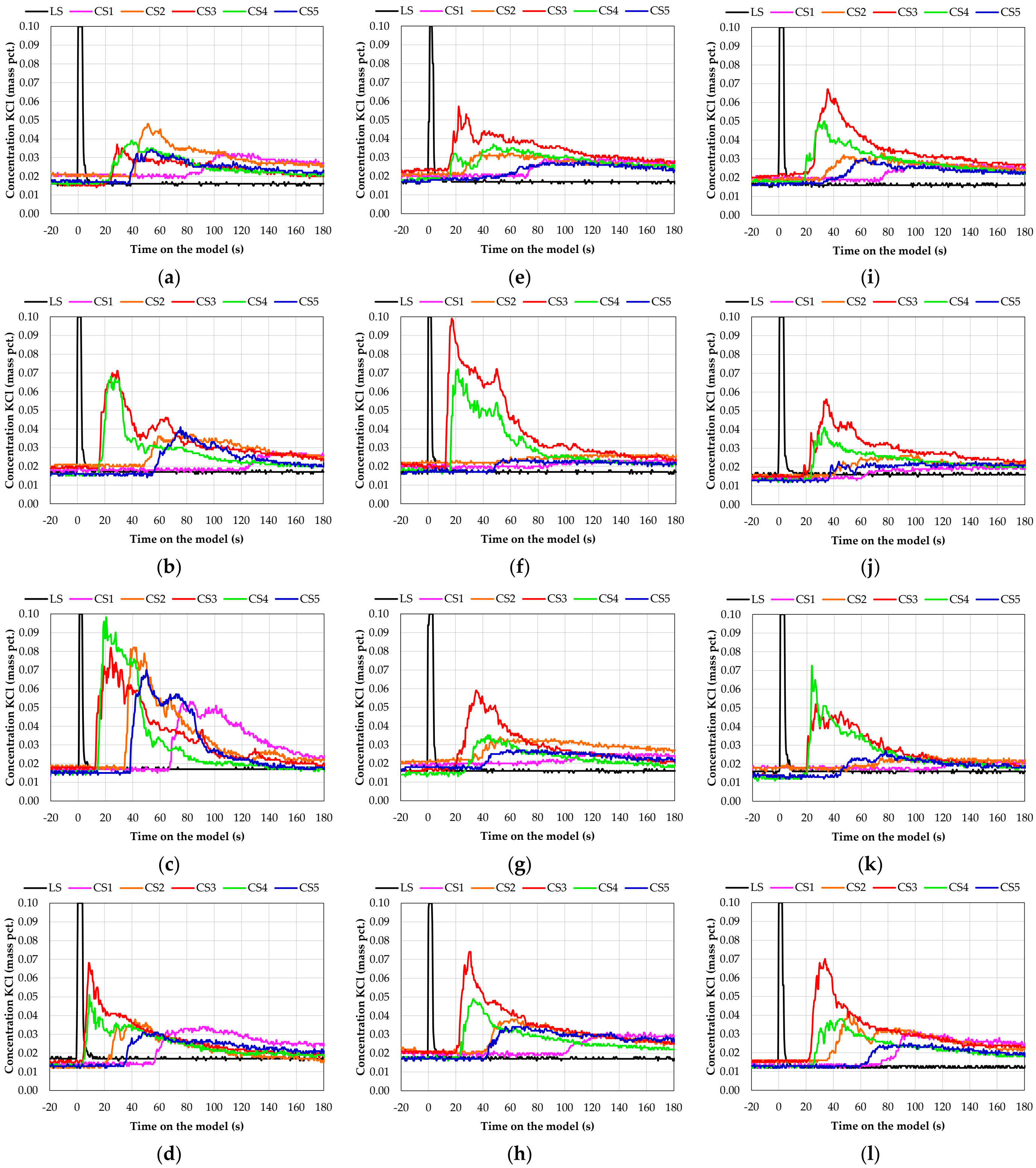

Figure 6. Characteristics RTD C-curves showing the dependence of concentration change on time for all of the modelled variants: (**a**) TI1-R1; (**b**) TI1-R2; (**c**) TI1-C; (**d**) TI1-F1; (**e**) TI2-R1; (**f**) TI2-R2; (**g**) TI2-R3; (**h**) TI2-C; (**i**) TI3-R1; (**j**) TI3-R2; (**k**) TI3-R3; (**l**) TI3-C3.

Table 4. Flow characteristics in physical experiments.

Variant	CS1 τ_{min} (s)	CS2 τ_{min} (s)	CS3 τ_{min} (s)	CS4 τ_{min} (s)	CS5 τ_{min} (s)	Ø τ_{min} (s)	v (%)	V_m/V (%)	V_p/V (%)	V_d/V (%)	V_p/V_d (-)
TI1-R1	95	41	20	19	41	43	71	57	25	18	1.34
TI1-R2	105	57	16	16	61	51	72	52	31	17	1.81
TI1-C	87	48	19	19	47	44	64	43	24	33	0.74
TI1-F1	65	27	4	5	39	28	91	54	16	30	0.51
TI2-R1	79	24	13	14	31	32	84	65	18	17	1.05
TI2-R2	81	39	14	16	47	40	69	55	22	23	0.98
TI2-R3	113	55	20	21	58	53	71	55	31	14	2.16
TI2-C	108	52	23	23	48	51	68	58	28	14	1.97
TI3-R1	65	22	15	12	29	28	75	56	16	28	0.56
TI3-R2	75	44	19	21	44	40	56	58	23	19	1.20
TI3-R3	104	50	16	18	59	49	73	53	28	20	1.39
TI3-C	93	43	25	25	57	49	58	59	27	14	1.99

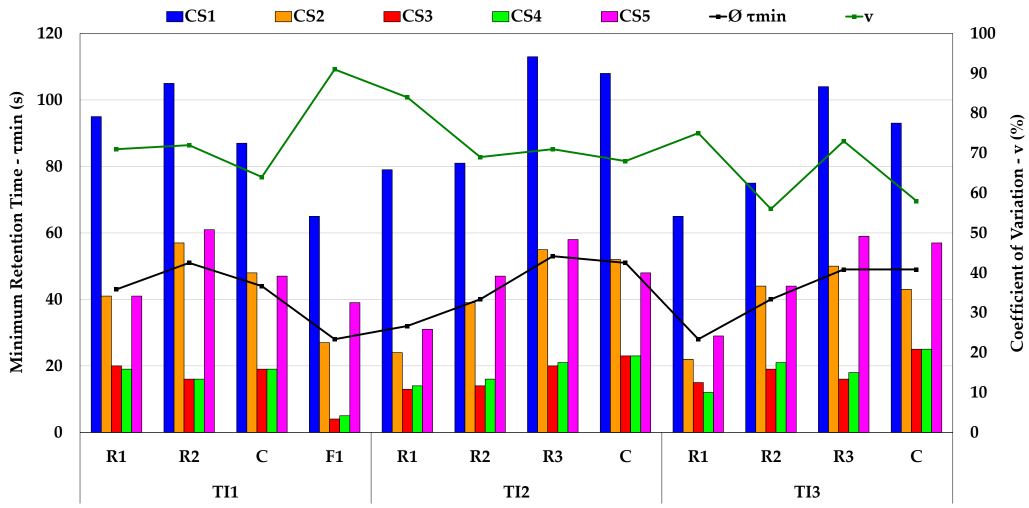

Figure 7. Comparison of average minimum retention times and their coefficients of variation for all modelled variants.

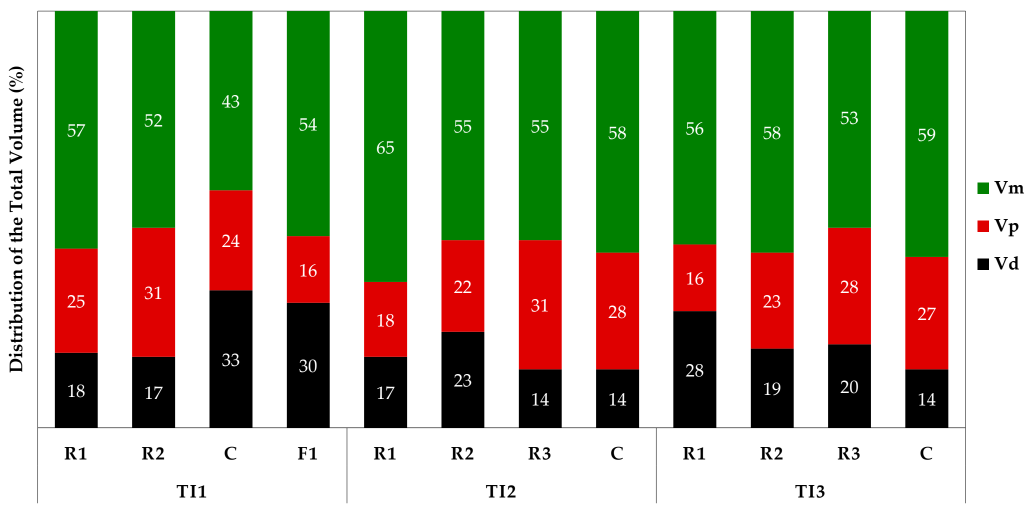

Figure 8. Graphical comparison of calculated proportions of individual volumes (V_m, V_p, V_d) in the tundish for all modelled variants.

TI1 with the F1 ladle shroud position caused an unwanted short-circuit flow on the nearest casting strands, CS3 and CS4. Therefore, the ladle shroud position F1 appears to be quite disadvantageous, and even risky. For TI2 and TI3, there was a prerequisite for reducing the dead zones in the areas around the first casting strand. It is encouraging that there was no short-circuit flow in the tested variants TI2 and TI3. TI1 performed best with the ladle shroud in the R2 position, as the values of the dead volume area were reduced by up to 17%. Also in ladle shroud in the R2 position, the largest areas were created for the bath flow a with plug flow (31%). TI2 performed best with the ladle shroud in the R3 position. With this ladle shroud position, there was a reduction in the dead volume of up to 14%. At the same time, the largest volume share was achieved with the plug flow (31%). TI3 performed best with the ladle shroud in the R2 position, and it achieved the lowest value of the coefficient of variation (56%). The average value of the coefficients of variation for all four variants when using this ladle shroud position reached (65.5%), which was the lowest of any position. However, the volume representation was better at ladle shroud position C, where the value of the volume with plug flow was 27% and the value of the dead volume was 14%. Overall, the coefficients of variation for the central positions of the ladle shroud reached, with some exceptions, lower values than for the positions that deviated from the center. Across all the variants in the physical modelling, the lowest coefficient of variation was achieved for TI3 (50%), and the average value of the coefficient of variation was also the lowest for this turbulence inhibitor (66% TI3, 70% TI2 and 73% TI1). In an asymmetric tundish, it is important to increase the minimum retention times in casting strands 2, 3, 4, 5 and, at the same time, reduce the minimum retention time on the farthest casting strand, CS1. This was partly achieved with regard to the coefficients of variation for TI3.

The V_p/V_d ratio proved to be a determining factor for the characteristics of the bath flow in the tundish (see Figure 9). A ratio of less than 1 means that the volume with plug flow is less than the dead volume. This is somewhat disadvantageous, since a sufficient volume with plug flow is desirable for the removal of non-metallic inclusions and other possible impurities.

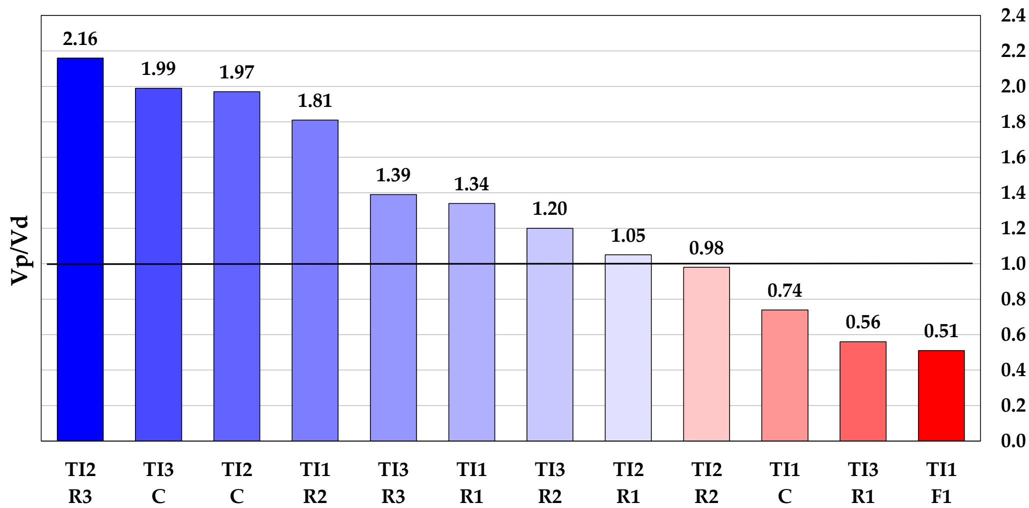

Figure 9. Ratio of volume with plug flow to dead volume for all variants.

For TI1, the V_p/V_d ratio reached the lowest absolute value (0.51). To an extent, this is related to the short-circuit flow that occurred in this variant (see Figure 6a). The highest V_p/V_d ratio (1.81) was achieved with the TI1 and ladle shroud position R2 combination. Ladle shroud R2 also had the largest areas with plug flow. For TI2, there were larger dead volume areas than volumes with plug flow for only one of the modelled variant, and the value of this ratio was close to 1 (0.98). The maximum absolute value of the V_p/V_d ratio (2.16) was also achieved with the TI2 and R3 ladle shroud position combination. When using TI3, a succession can be seen in relation to the position of the ladle shroud. The highest V_p/V_d ratio was achieved at the central position of the ladle shroud (C). As the ladle shroud moved further from the center of the turbulence inhibitor, successively positioned at R3, R2 and R1, the V_p/V_d ratio decreased. The highest V_p/V_d ratio (1.99) was thus achieved at the center ladle shroud position (C). For TI3, it is important to note that when the flow impacted the center of the turbulence inhibitor, i.e., the top of the convex bottom, and was further evenly distributed. Also, for this turbulence inhibitor with the central ladle shroud position, the bottom has a longer life due to its raised center.

3.3. Optical Recording of the Flow Characteristics Inside the Tundish Model

The results from the physical modelling were also evaluated through the visualization of the flow in the model of the tundish. The dyed liquid method was used to achieve this: an impulse of the contrast substance, an aqueous solution of $KMnO_4$, was injected into the ladle shroud. During the visualization, photos of the behavior of the bath inside the model were taken, making it possible to more closely evaluate the characteristics of the fluid flow. The influence of the shape of the turbulence inhibitor and the position of the ladle shroud in relation to the turbulence inhibitor was monitored. Images were taken 10, 30, 60 and 100 s after the dye injection, as shown in Figures 10–12.

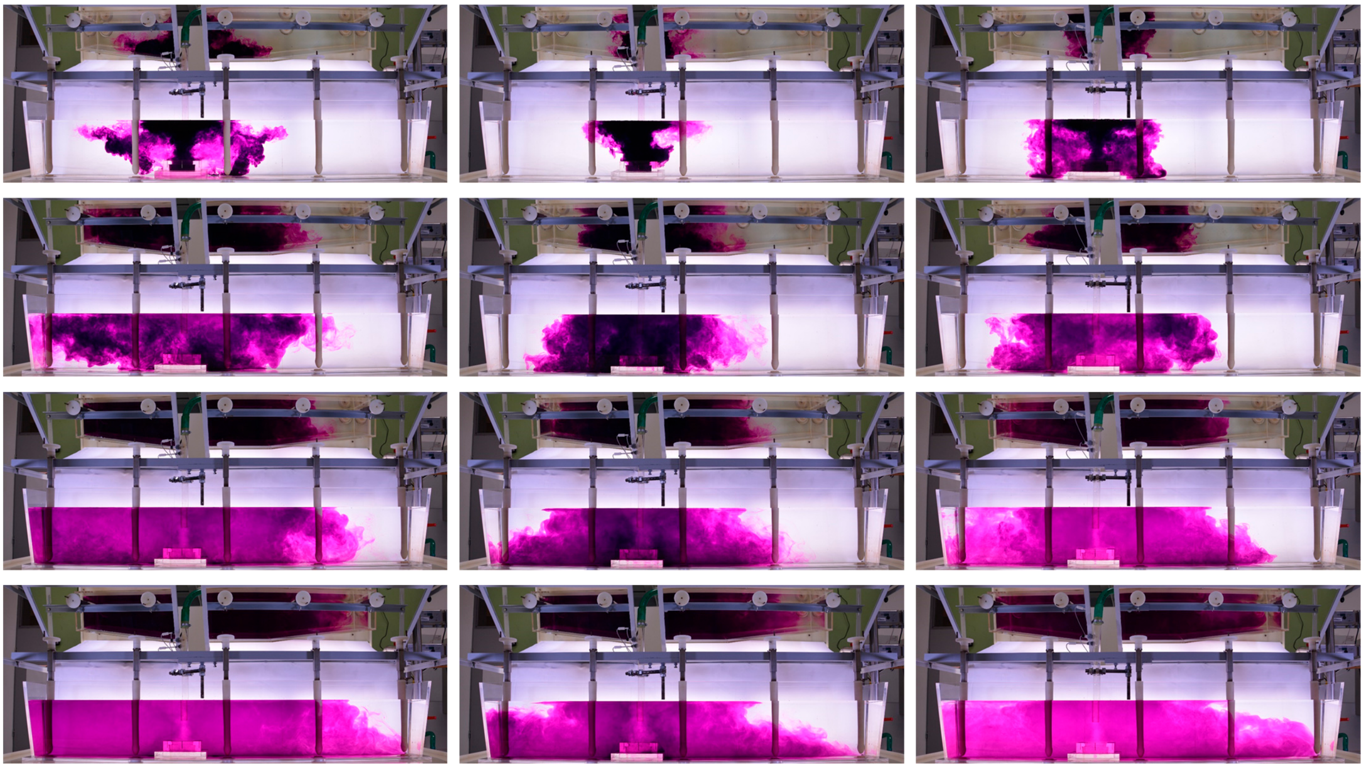

(**a**) (**b**) (**c**)

Figure 10. Visualization of the bath flow in the tundish model 10, 30, 60 and 100 s after injection for the modelled variants: (**a**) TI1-R1; (**b**) TI1-R2; (**c**) TI1-F1.

In the visualization photos, the primary function of these types of the turbulence inhibitors (TI1, TI2, TI3), the redirection of the flow of water, falling on the bottom of the turbulence inhibitor, back to the surface, can be observed. The exception is the combination of the ladle shroud in position R1 and TI1 (see Figure 10a, 10 s). This arrangement confirms the above conclusion, that there is a short-circuit flow, as the concentration was already detected in the nearest casting strands, CS3 and CS4, during the impulse of the contrast substance into the ladle shroud. The different colors of the bath also show where the bath flows at the highest speed. At 100 s, there was no complete mixing of the bath in the entire volume of the tundish for TI1. For TI2 and TI3, the contrast solution was overall faster, and mixing was observed in a significantly larger volume in the tundish compared to TI1.

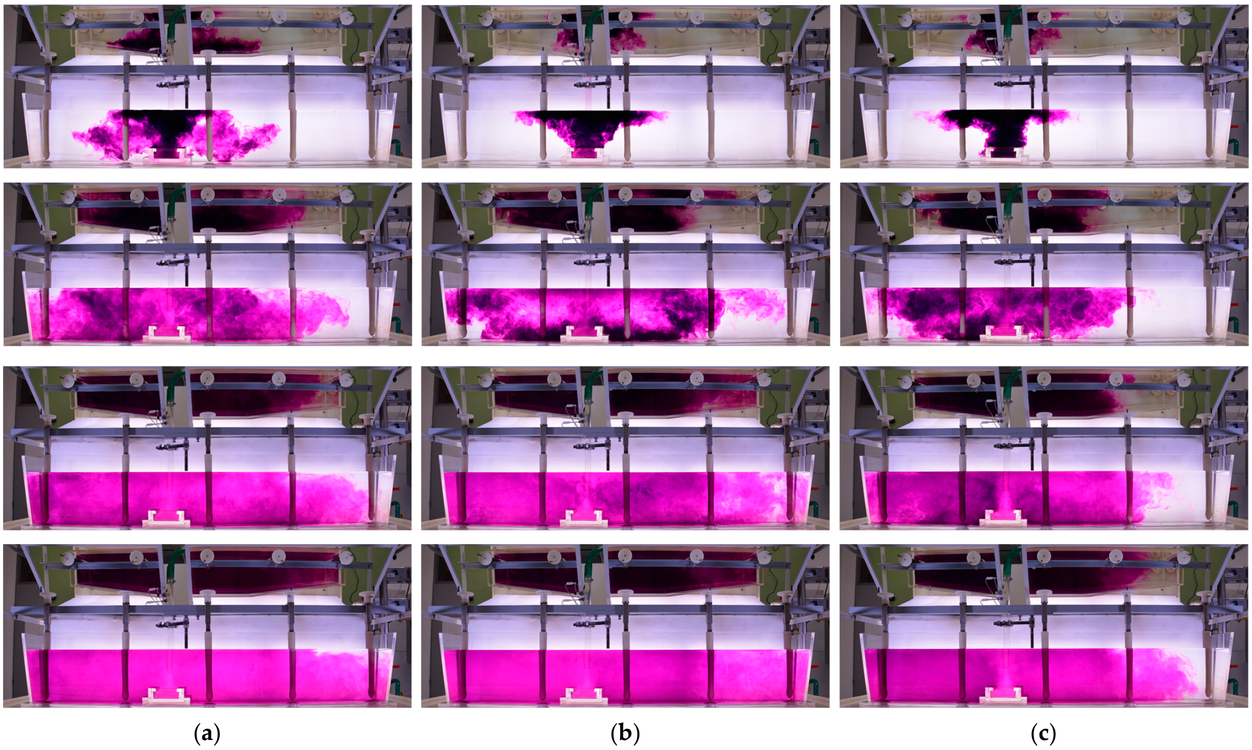

Figure 11. Visualization of the bath flow in the tundish model 10, 30, 60 and 100 s after injection for the modelled variants: (**a**) TI2-R1; (**b**) TI2-R2; (**c**) TI2-F1.

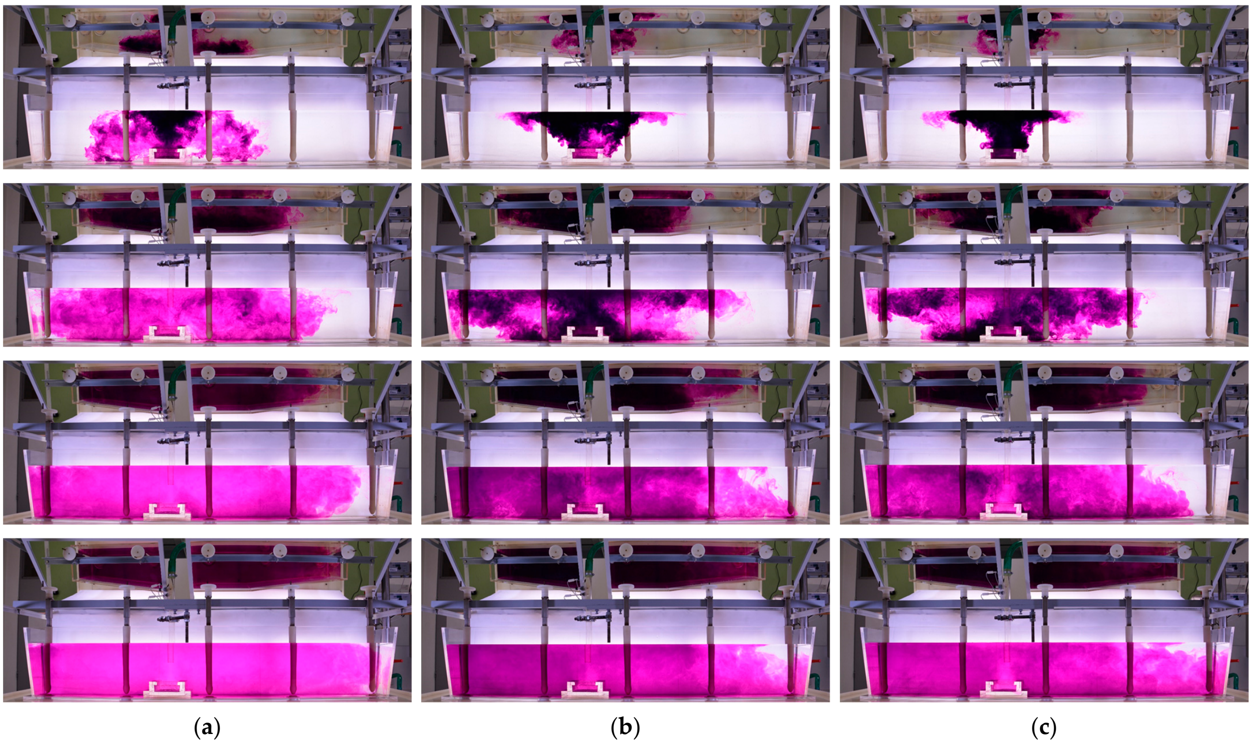

Figure 12. Visualization of the bath flow in the tundish model at 10, 30, 60 and 100 s after injection for the modelled variants: (**a**) TI3-R1; (**b**) TI3-R2; (**c**) TI3-F1.

3.4. Evaluation of the Flow Characteristics in the Numerical Simulations

Based on the numerical simulations, an evaluation of the results from the transient calculation of RTD curves was performed using the species model, where a permanent change in concentration was monitored. The results were in the form of F-curves, showing the dependence of the permanent change in concentration on time (see Figure 13).

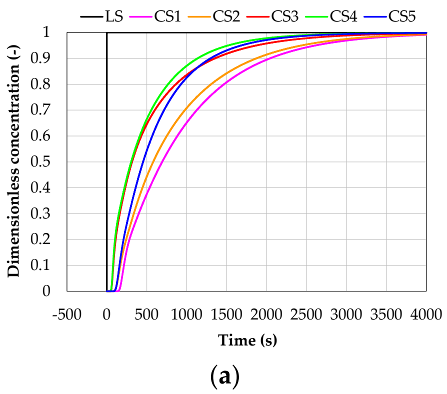

Figure 13. Characteristics F-curves for the numerical simulations variants: (**a**) TI1-C; (**b**) TI2-C; (**c**) TI3-C.

The calculated F-curves were recalculated into C-curves using derivation (see Figure 14); the data from the C-curves were used to check the determination of the minimum retention times from the F-curves.

$$C = dF/d\tau \tag{8}$$

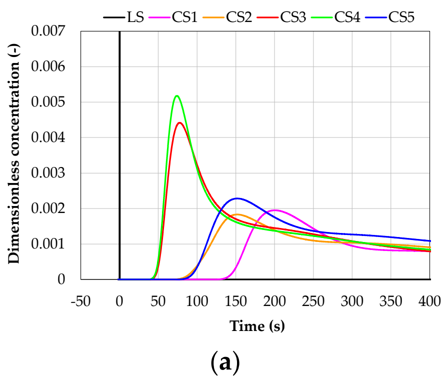

Figure 14. C-curves recalculated using the derivation of F-curves for variants: (**a**) TI1-C; (**b**) TI2-C; (**c**) TI3-C.

The established minimum retention times for a given casting strands, the average value from all five casting strands and their coefficients of variation from the numerical simulations are shown in the Table 5. In the numerical simulations, for TI1, the minimum retention times were first detected for the nearest strands, CS3 and CS4 (45 and 44 s), in approximately twice the time for CS2 and CS5 (79 and 85 s) and lastly, as expected, for the furthest strand, CS1 (135 s). Overall, this variant had a relatively low coefficient of variation (48%). The minimum retention times for CS3 and CS4 for T12 were similar to those for TI1 (44 and 45 s); however, there was a reduction in the minimum retention times for CS2 and CS5 (54 and 59 s) and even more so for CS1 (120 s), which led to the overall equalization of the steel flow in the tundish. This variant also showed a low coefficient of variation (49%). For TI3, similar minimum retention times to T12 were detected for CS2, CS3, CS4 and CS5 (60, 49, 46 and 55 s). However, there was a relatively significant increase in times for CS1 (155 s), which was also reflected in an increase in the coefficient of variation (63%).

Table 5. Minimum retention times and their coefficients of variation for variants in the numerical simulations.

Variant	CS1 τ_{min} (s)	CS2 τ_{min} (s)	CS3 τ_{min} (s)	CS4 τ_{min} (s)	CS5 τ_{min} (s)	Ø τ_{min} (s)	v (%)
TI1-C	135	79	45	44	85	78	48
TI2-C	120	54	44	45	59	64	49
TI3-C	155	60	49	46	55	73	63

3.5. Comparison of the Results of the Physical Experiments and Numerical Simulations

Table 6 shows the minimum retention times from the results of the physical experiments for the selected variants, their conversion to the conditions of the prototype (time scale Mτ = 0.5) and the minimum retention times determined from the results of the numerical simulations. These results also show the permanent change in concentration of the impulse and the transformation of the obtained F-curves into C-curves. When using TI2 and TI3, the converted minimum retention times of the prototype were always higher than the minimum retention times found in the numerical simulations. When using TI1, the converted minimum retention times of the prototype were also higher, with the exception of casting strands closest to the ladle shroud, CS3 and CS4, where the higher minimum retention times were equal to those from numerical simulations.

Table 6. Comparison of minimum retention times from the physical experiments and numerical simulations.

Variant	Conditions	CS1 τ_{min} (s)	CS2 τ_{min} (s)	CS3 τ_{min} (s)	CS4 τ_{min} (s)	CS5 τ_{min} (s)	Ø τ_{min} (s)
TI1-C	Model	87	48	19	19	47	44
	Prototype	174	96	38	38	94	88
	NS	135	79	45	44	85	78
TI2-C	Model	108	52	23	23	48	51
	Prototype	216	104	46	46	96	102
	NS	120	54	44	45	59	64
TI3-C	Model	93	43	25	25	57	49
	Prototype	186	86	50	50	114	98
	NS	155	60	49	46	55	73

Deviations in the values of the minimum retention times in the physical and numerical model can be explained by different influences, such as using two different methods to determine retention times. This is the reason for implementing an instantaneous impulse (Dirac impulse—C-curve) in the physical experiments, in contrast to permanent change of marker concentration (Heaviside unit step—F-curve) in the numerical simulations. In the numerical simulations, the selected turbulence model (e.g., k-epsilon, k-omega), in some cases, affected the resulting retention time values.

Numerical modelling confirmed the results from the physical modelling, and with regard to determining the minimum retention times on individual casting strands, the verification of the results can be considered sufficiently determining. Within all modelled variants, the minimum retention times were detected first on CS3 and CS4, then on CS2 and CS5, and lastly on the furthest, CS1.

4. Conclusions

In the case of this asymmetric tundish, it is important to increase the values of the minimum retention times for casting strands 2, 3, 4 and 5, and, at the same time, reduce the minimum retention time for casting strand 1. This was partially achieved in regard to the the coefficients of variation by using TI3. The V_p/V_d ratio has proven to be a determining factor for the characteristics of the flow of the bath in the tundish. In regard to the removal of non-metallic inclusions and other possible impurities, it is advantageous for the value of the ratio to be as large as possible. In accordance with the literature, the shape of the turbulence inhibitor and the position of the ladle shroud in relation to the turbulence inhibitor appeared to be crucial parameters influencing the characteristics of the steel flow in the tundish. It is important that the entire volume of the flow falls inside the turbulence inhibitor and to avoid positions where the flow falls mainly on the front edge of the turbulence inhibitor. As part of the model research solution, geometric modifications to existing turbulence inhibitors and other technological parameters used in the operating conditions were proposed and verified, in order to optimize steel flow in the tundish. The optimization of the steel flow in the tundish using TI3 has been proven through physical and numerical modelling. The comparison of the results of physical and numerical modelling is an effective and optimal variant of model research, providing a modern approach to solving practical industrial problems.

Author Contributions: Conceptualization and methodology, characterization, visualization and writing—original draft, J.W.; methodology, characterization and writing—review and editing, M.T.; writing—review and editing, M.V., M.M., J.C. (Jiří Cupekand), T.H., J.C. (Jiří Cibulka) and J.R.; methodology, characterization and writing—review and editing, K.M. All authors have read and agreed to the published version of the manuscript.

Funding: This study was conducted with the support of a student grant competition run by the VSB—Technical University of Ostrava, project number SP2023/034—Research and Development of Composite Multifunctional Materials for Sustainable Progress.

Data Availability Statement: Not applicable.

Acknowledgments: This research was undertaken thanks to project No. CZ.02.1.01/0.0/0.0/17_049/0008399 of the EU, and CR financial funds provided by the Operational Programme Research, Development and Education, Call 02_17_049 Long-Term Intersectoral Cooperation for ITI, Managing Authority: Czech Republic—Ministry of Education.

Conflicts of Interest: Markéta Tkadlečková; Tomáš Huczala and Jiří Cibulka were employed by the company TŘINECKÉ ŽELEZÁRNY, a.s. The authors declare no conflict of interest. The funders had no role in the design of this study; in the collection, analyses or interpretation of data; in the writing of the manuscript; or in the decision to publish the results.

References

1. Louhenkilpi, S. Treatise on Process Metallurgy. In *Continuous Casting of Steel*; Elsevier: Amsterdam, The Netherlands, 2014; Volume 3, pp. 373–434.
2. Michalek, K. *Využití Fyzikálního a Numerického Modelování pro Optimalizaci Metalurgických Procesů*; VŠB—Technická Univerzita Ostrava: Ostrava, Czech Republic, 2001; p. 125. (In Czech)
3. Sahai, Y. Metallurgical and Materials Transactions B. In *Tundish Technology for Casting Clean Steel: A Review*; Springer: New York City, NY, USA, 2016; Volume 47, pp. 2095–2106.
4. Huang, W.; Chang, S.; Zou, Z.; Shao, L.; Qu, Y.; Li, B. Modeling of Flow Behaviors in a Swirling Flow Tundish for the Deep Cleaning of Molten Steel. *Steel Res. Int.* **2021**, *92*, 2100012. [CrossRef]
5. Delgado Ramirez, O.S.; Torres-Alonso, E.; Ramos Banderas, J.A.; Arreola, S.A.; Hernandez Bocanegra, C.A.; Tellez Martinez, J.S. Thermal and Fluid Dynamic Optimization of a Five Strand Asymmetric Delta Shaped Billet Caster Tundish. *Steel Res. Int.* **2018**, *89*, 1700428. [CrossRef]
6. Zhang, B.; Liu, F.; Zhu, R.; Zhu, J. Effects of Multiple-Hole Baffle Arrangements on Flow Fields in a Five-Strand Asymmetric Tundish. *Materials* **2020**, *13*, 5129. [CrossRef] [PubMed]
7. Yadav, J.N.; Singh, N.P. Experimental and Simulation Analysis of Physical Water Model through Tracer Injection under Various Baffles and Turbulence Inhibitor Conditions for Developing the Fluid Flow Parameters and Inclusion Removal Rates in Tundish. *Biointerface Res. Appl. Chem.* **2022**, *12*, 6361–6381.
8. Gupta, V.K.; Jha, P.K.; Jain, P.K. Modeling of Wall Shear Stress Induced Inclusion Transport and Removal in Multi-Strand Tundish. *ISIJ Int.* **2021**, *61*, 2445–2456. [CrossRef]
9. Morales, R.D.; Guarneros, J.; Najera-Bastida, A.; Rodriguez, J. Control of Two-Phase Flows during Startup Operations of Casting Sequences in a Billet Tundish. *JOM* **2018**, *70*, 2103–2108. [CrossRef]

10. Morales, R.D.; Guarneros, J.; Chattopadhyay, K.; Najera-Bastida, A.; Rodriguez, J. Fluid Flow Control in a Billet Tundish during Steel Filling Operation. *Metals* **2019**, *9*, 394. [CrossRef]
11. Ling, H.; Xu, R.; Wang, H.; Chang, L.; Qiu, S. Multiphase Flow Behavior in a Single-Strand Continuous Casting. *ISIJ Int.* **2020**, *60*, 499–508. [CrossRef]
12. Xu, R.; Ling, H.; Wang, H.; Chang, L.; Qiu, S. Investigation on the control of multiphase flow behavior in a continuous casting tundish during ladle change. *Metall. Res. Technol.* **2020**, *117*, 619. [CrossRef]
13. Jin, Y.; Dong, X.; Yang, F.; Cheng, C.; Li, Y.; Wang, W. Removal Mechanism of Microscale Non-Metallic Inclusions in a Tundish with Multi-Hole-Double-Baffles. *Metals* **2018**, *8*, 611. [CrossRef]
14. Bartosiewicz, M.; Cwudziński, A. Influence of Multi-Hole Filter Modification on the Flow Hydrodynamic Structure and Refining Process of Liquid Steel in the One-Strand Tundish. *Arch. Metall. Mater.* **2019**, *64*, 71–78. [CrossRef]
15. Wang, Q.; Liu, Y.; Huang, A.; Yan, W.; Gu, H.; Li, G. CFD Investigation of Effect of Multi-hole Ceramic Filter on Inclusion Removal in a Two-Strand Tundish. *Met. Mater. Trans. B* **2020**, *51*, 276–292. [CrossRef]
16. Wang, Q.; Tan, C.; Huang, A.; Yan, W.; Gu, H.; He, Z.; Li, G. Numerical Simulation on Refractory Wear and Inclusion Formation in Continuous Casting Tundish. *Met. Mater. Trans. B* **2021**, *52*, 1344–1356. [CrossRef]
17. Liu, C.; Xiao, A.; He, Z.; Yan, W.; Li, G.; Wang, Q. Numerical Investigation on Motion and Removal of Inclusions in Continuous Casting Tundish with Multiorifice Filter. *Steel Res. Int.* **2022**, *93*, 2100818. [CrossRef]
18. Sheng, D.-Y. Mean Age Theory in Continuous Casting Tundish. *Met. Mater. Trans. B* **2022**, *53*, 2735–2752. [CrossRef]
19. Sheng, D.-Y.; Chen, D. Comparison of Fluid Flow and Temperature Distribution in a Single-Strand Tundish with Different Flow Control Devices. *Metals* **2021**, *11*, 796. [CrossRef]
20. Michalek, K.; Gryc, K.; Tkadlečková, M.M.; Bocek, D. Model Study of Tundish Steel Intermixing and Operational Verification. *Arch. Metall. Mater.* **2012**, *57*, 291–296. [CrossRef]
21. Cwudziński, A. Numerical and Physical Modeling of Liquid Steel Flow Structure for One Strand Tundish with Modern System of Argon Injection. *Steel Res. Int.* **2017**, *88*, 1600484. [CrossRef]
22. Cwudziński, A. Mathematical Simulation and Water Modelling of Liquid Steel Interaction with an Argon Bubble Curtain in a One-Strand Continuous Casting Tundish. *J. S. Afr. Inst. Min. Metall.* **2018**, *118*, 545–554. [CrossRef]
23. Walek, J.; Michalek, K.; Tkadlečková, M.; Saternus, M. Modelling of Technological Parameters of Aluminium Melt Refining in the Ladle by Blowing of Inert Gas through the Rotating Impeller. *Metals* **2021**, *11*, 284. [CrossRef]
24. Mazumdar, D.; Evans, J.W. *Modeling of Steelmaking Processes*; CRC Press, Taylor & Francis Group: Boca Raton, FL, USA, 2010; p. 463.
25. Tkadlečková, M.; Walek, J.; Michalek, K.; Huczala, T. Numerical Analysis of RTD Curves and Inclusions Removal in a Multi-Strand Asymmetric Tundish with Different Configuration of Impact Pad. *Metals* **2020**, *10*, 849. [CrossRef]
26. Nastac, L.; Pericleous, K.; Sabau, A.S.; Zhang, L.; Thomas, B.G. *CFD Modeling and Simulation in Materials Processing 2018*; The Minerals, Metals & Materials Series; Springer: Cham, Switzerland, 2018; p. 241.
27. Zhang, J.; Yang, S.; Li, J.; Tang, H.; Jiang, Z. The Effect of a Dissipative Ladle Shroud on Mixing in Tundish: Mathematical and Experimental Modelling. *High Temp. Mater. Proc.* **2017**, *37*, 25–32. [CrossRef]
28. Harnsihacacha, A.; Piyapaneekoon, A.; Kowitwarangkul, P. Physical water model and CFD studies of fluid flow in a single strand tundish. *Mater. Today Proc.* **2018**, *5*, 9220–9228. [CrossRef]
29. Lopez-Ramirez, S.; Barreto, J.d.J.; Palafox-Ramos, J.; Morales, R.D.; Zacharias, D. Modelling Study of the Influence of Turbulence Inhibitors on the Molten Steel Flow, Tracer Dispersion, and Inclusion Trajectories in Tundishes. *Met. Mater. Trans. B* **2001**, *32*, 615–627. [CrossRef]
30. Morales, R.D.; Lopez-Ramirez, S.; Palafox-Ramos, J.; Zacharias, D. Mathematical simulation of effects of flow control devices and buoyancy forces on molten steel flow and evolution of output temperatures in tundish. *Ironmak. Steelmak.* **2001**, *28*, 33–43. [CrossRef]